Poster #7821

Plasma-based comprehensive epigenomic profiling enables multiplexed prediction of target gene expression and detection of resistance mechanisms

Nicole Kramer[1], Jonathan Beagan[1], Aparna Gorthi[1], Daniel Karl[1], Humphrey Gardner[1], Praful Ravi[2], Rashad Nawfal[2], Anthony D'Ippolito[1], Sylvan Baca[2], Travis Clark[1], Karl Semaan[2], Khoi Nguyen[1], Marc Eid[2], Jacob Berchuck[3], Kristian Cibulskis[1]; Matthew Eaton[1], J. Carl Barrett[1]

[1]Precede Biosciences, Boston, MA; [2]Dana-Farber Cancer Institute, Boston, MA, USA; [3]Winship Cancer Institute of Emory University, Atlanta, GA

BACKGROUND

Prostate cancer progression to metastatic castration-resistant disease (mCRPC) and treatment-emergent neuroendocrine prostate cancer (NEPC) represents a critical clinical challenge marked by lineage plasticity, therapeutic resistance, and poor prognosis. As novel targeted therapies, including drug, radio-, and immune-conjugates, advance toward broad clinical implementation, there is an urgent need for scalable, minimally invasive diagnostics capable of resolving gene expression programs to guide patient selection and therapeutic monitoring. Conventional diagnostic platforms are limited by restricted access to contemporaneous tissue, tumor heterogeneity, limited multiplexing capacity, and challenges in longitudinal profiling. To address these limitations, we applied a comprehensive epigenomics liquid biopsy[1] and machine learning platform to infer tumor gene expression, delineate lineage plasticity, and reveal therapeutically relevant molecular programs and resistance mechanisms from only 1 mL of plasma.

METHODS

1 mL of plasma from a pan-cancer cohort of patients (94 prostate adenocarcinoma [PRAD], 17 neuroendocrine prostate cancer [NEPC], 55 non-small cell lung cancer [NSCLC], 65 small cell lung cancer [SCLC], 2 large cell lung cancer [LCLC], 150 breast cancer [BRCA], 21 gastroesophageal cancer [GEA], 17 additional neuroendocrine carcinomas (8 colorectal [COADNEC], 5 pancreatic [PANCNEC], 3 lung [LCLC], 1 gastroesophageal [GENEC]), and 5 ovarian cancer [OVAR]) was profiled using Precede Biosciences liquid biopsy platform. All samples were assessed for the expression of therapeutically relevant targets using models to predict gene expression from plasma epigenomic signals[2,3]. In prostate cancer, samples were further evaluated for the extent of neuroendocrine (NE) transformation, a key mechanism of lineage plasticity and therapeutic resistance. Immunohistochemistry (IHC) for DLL3 (Ventana SP347) and CEACAM5 (Thermo ZR370) was performed according to manufacturers' protocols and scored by a board-certified pathologist using established criteria.

METHODS

Figure 1. Plasma epigenomic platform

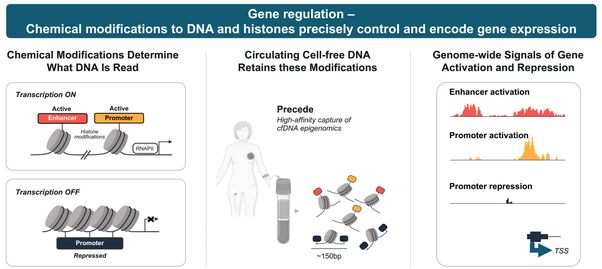

Figure 2. Precede Bio Insight™ identifies canonical NEPC and PRAD marker genes and transcriptional programs

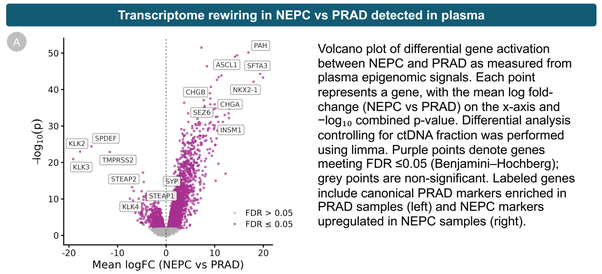

Volcano plot of differential gene activation between NEPC and PRAD as measured from plasma epigenomic signals. Each point represents a gene, with the mean log fold-change (NEPC vs PRAD) on the x-axis and $-\log_{10}$ combined p-value. Differential analysis controlling for ctDNA fraction was performed using limma. Purple points denote genes meeting FDR ≤0.05 (Benjamini–Hochberg); grey points are non-significant. Labeled genes include canonical PRAD markers enriched in PRAD samples (left) and NEPC markers upregulated in NEPC samples (right).

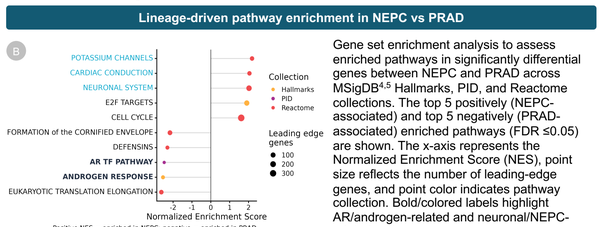

Gene set enrichment analysis to assess enriched pathways in significantly differential genes between NEPC and PRAD across MSigDB[4,5] Hallmarks, PID, and Reactome collections. The top 5 positively (NEPC-associated) and top 5 negatively (PRAD-associated) enriched pathways (FDR ≤0.05) are shown. The x-axis represents the Normalized Enrichment Score (NES), point size reflects the number of leading-edge genes, and point color indicates pathway collection. Bold/colored labels highlight AR/androgen-related and neuronal/NEPC-related pathways.

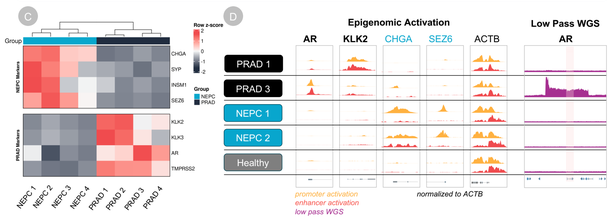

Heatmap of plasma epigenomic activation (promoter) at canonical NEPC and PRAD markers. A representative subset of 4 samples per group is shown, with columns clustered hierarchically. Rows are grouped by marker class (NEPC, PRAD).

Signal tracks display normalized cfChIP-seq read coverage at promoter/enhancers of select marker genes from representative PRAD, NEPC and healthy donor plasma. NEPC-associated *(CHGA, SEZ6)* and PRAD-associated *(KLK2, AR)* loci illustrate differential histone modification enrichment between disease groups, with a male healthy donor serving as a non-cancer reference baseline. Low-pass whole-genome sequencing (lpWGS) copy number profile around the AR locus and flanking genes on chromosome X. Read-depth–derived copy number illustrates focal amplification of AR in PRAD 3.

Figure 3. Plasma-based quantitative NEPC score distinguishes NEPC from PRAD and captures mixed lineage disease

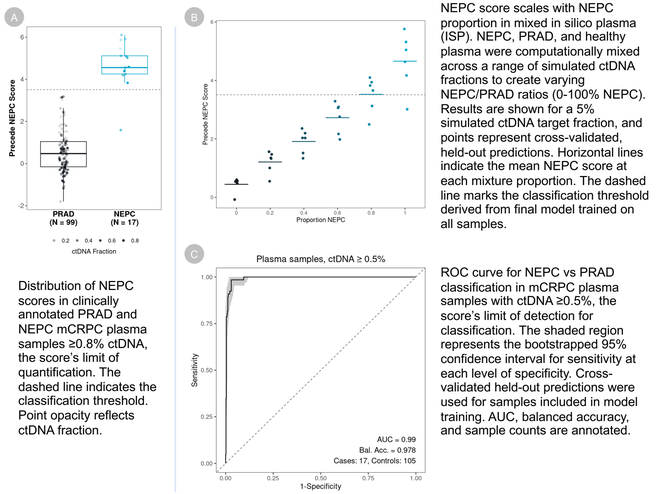

The NEPC score is a quantitative epigenomic score that integrates NEPC- and PRAD-associated features to measure the degree of neuroendocrine differentiation in metastatic castration-resistant prostate cancer (mCRPC) plasma.

Distribution of NEPC scores in clinically annotated PRAD and NEPC mCRPC plasma samples ≥0.8% ctDNA, the score's limit of quantification. The dashed line indicates the classification threshold. Point opacity reflects ctDNA fraction.

NEPC score scales with NEPC proportion in mixed in silico plasma (ISP). NEPC, PRAD, and healthy plasma were computationally mixed across a range of simulated ctDNA fractions to create varying NEPC/PRAD ratios (0-100% NEPC). Results are shown for a 5% simulated ctDNA target fraction, and points represent cross-validated, held-out predictions. Horizontal lines indicate the mean NEPC score at each mixture proportion. The dashed line marks the classification threshold derived from final model trained on all samples.

ROC curve for NEPC vs PRAD classification in mCRPC plasma samples with ctDNA ≥0.5%, the score's limit of detection for classification. The shaded region represents the bootstrapped 95% confidence interval for sensitivity at each level of specificity. Cross-validated held-out predictions were used for samples included in model training. AUC, balanced accuracy, and sample counts are annotated.

Application of AR and NE score on a cohort of samples highlights PRAD, NEPC and mixed lineages

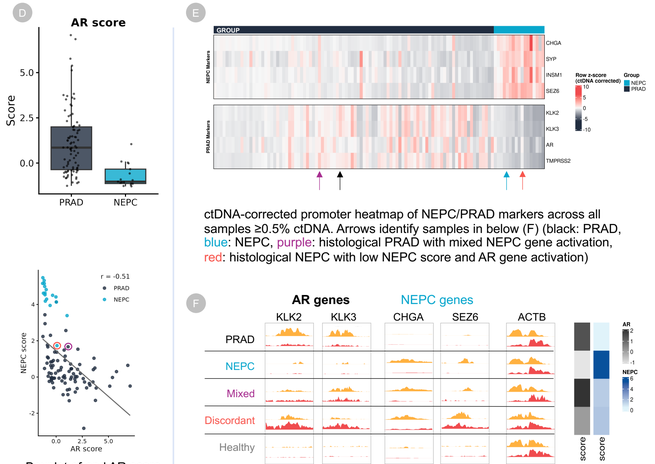

Boxplot of and AR score (ctDNA ≥1.8%) stratified by cohort and scatterplot of NEPC vs AR score with Pearson correlation. Red and purple highlights identify mixed and discordant samples illustrated in (E) and (F).

ctDNA-corrected promoter heatmap of NEPC/PRAD markers across all samples ≥0.5% ctDNA. Arrows identify samples in below (F) (black: PRAD, blue: NEPC, purple: histological PRAD with mixed NEPC gene activation, red: histological NEPC with low NEPC score and AR gene activation)

Left: epigenomic tracks at *KLK2, KLK3, CHGA, SEZ6* for four samples — typical PRAD (24% ctDNA), typical NEPC (22% ctDNA), mixed-histology PRAD (20% ctDNA), and AR-retaining NEPC (43% ctDNA).
Right: heatmap of AR/NEPC scores for those four samples.

Figure 4. Multiplexed assessment of precision medicine target expression in PRAD vs NEPC

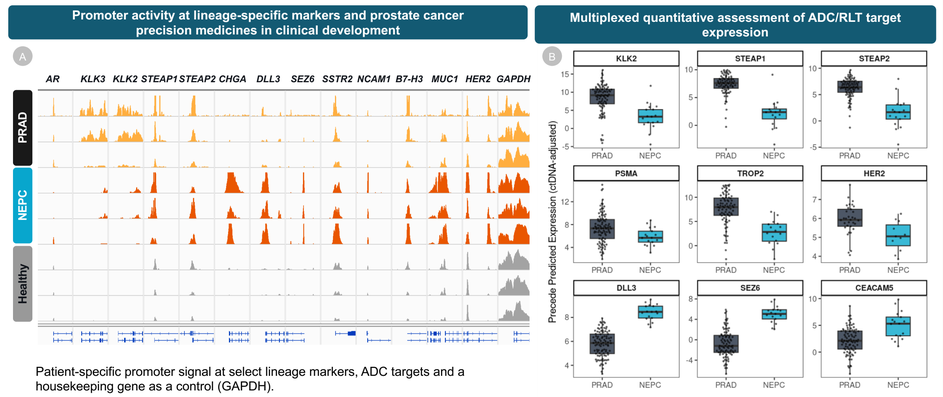

Patient-specific promoter signal at select lineage markers, ADC targets and a housekeeping gene as a control (GAPDH).

Box plots of predicted expression using Precede Insight™ of emerging ADC/RLT targets in prostate cancer. Quantitative scores recapitulate expected dynamic range within PRAD and NEPC cohorts.

Figure 5. Validation of Plasma-based Expression Measurements

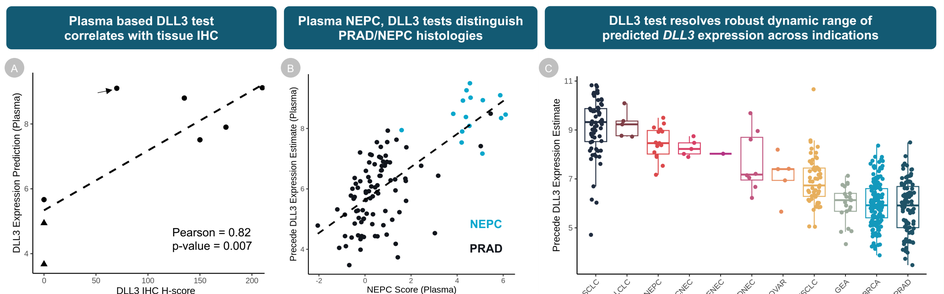

(A) Predicted *DLL3* expression from plasma shows robust agreement with DLL3 positive/negative status from tumor tissue IHC. Scatter plot/regression line indicate the correlation between plasma-based *DLL3* predictions (y-axis) and protein-level DLL3 scores from tissue IHC (x-axis). IHC is quantified via mean of cytoplasmic, membrane H scores. Triangles denote samples with ctDNA levels < 1%. Arrow denotes sample with highest predicted *INSM1* expression, suggesting tissue section stained may be an underestimate of global DLL3+ tumor burden. Predictions are corrected for ctDNA abundance.

(B) Independent NEPC (x-axis), *DLL3* expression (y-axis) scores correlate across prostate cancer patient cohort.

(C) Predicted *DLL3* expression exhibits expected dynamic ranges across multiple cancer indications, supporting a pan-cancer application of the DLL3 test.

***CEACAM5* gene expression predictions correlate with tissue IHC**

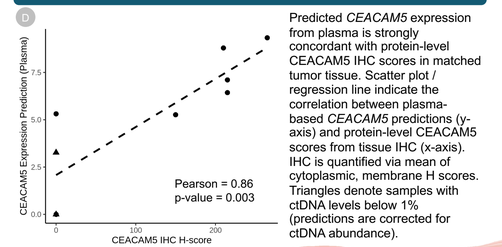

Predicted *CEACAM5* expression from plasma is strongly concordant with protein-level CEACAM5 IHC scores in matched tumor tissue. Scatter plot / regression line indicate the correlation between plasma-based *CEACAM5* predictions (y-axis) and protein-level CEACAM5 scores from tissue IHC (x-axis). IHC is quantified via mean of cytoplasmic, membrane H scores. Triangles denote samples with ctDNA levels below 1% (predictions are corrected for ctDNA abundance).

CONCLUSIONS

Plasma-based epigenomic profiling delineated a continuum of neuroendocrine differentiation, uncovering molecular states associated with therapeutic response and resistance.

The NEPC test distinguished PRAD from NEPC while capturing intermediate, heterogeneous states with concurrent lineage programs.

The assay further enables multiplexed assessment of tumor gene expression programs of key therapeutic targets such as *DLL3* with a dynamic range consistent with orthogonal tissue-based measurements.

Collectively, these findings underscore the potential of a minimally invasive, comprehensive epigenomics platform to deliver real-time, gene expression–level insights into tumor evolution and target expression, thereby guiding therapeutic decision-making.

References
1) Baca et al., *Nature Medicine* 2023
2) Nguyen K et al., *AACR* 2025
3) Nguyen K, Karl D, Beagan J, et al., ESMO 2025
4) Subramanian, Tamayo, et al., *PNAS* 2005
5) Liberzon et al., *Cell Systems* 2015

Contact J. Carl Barrett, PhD
Precede Biosciences
Email: carl.barrett@precede.bio